

# Quantifying small changes in brain ventricular volume using non-rigid registration

Mark Holden, Julia A. Schnabel, and Derek L. G. Hill

Computational Imaging Science Group, Division of Radiological Sciences and Medical Engineering, Guy's, King's and St. Thomas' School of Medicine, Guy's Hospital, King's College London, UK  
{mark.holden,julia.schnabel,derek.hill}@kcl.ac.uk

**Abstract.** Non-rigid registration can automatically quantify small changes in volume of anatomical structures over time by means of segmentation propagation. Here we use a non-rigid registration algorithm based on optimising normalised mutual information to quantify small changes in brain ventricular volume in MR images of a group of five patients treated with growth hormone replacement therapy and a control group of six volunteers. The lateral ventricles are segmented from each subject image by registering the brainweb image [1] which has this structure delineated. The mean (standard deviation) volume change measurements are 1.09cc (0.73cc) for the patient group and 0.08cc (0.62cc) for the volunteer group, this difference is statistically significant at the 1% level. We validate our volume change measurements by comparing them to previously published results obtained by visual inspection of difference images, and demonstrate high rank correlation coefficient ( $\rho = 0.7$ ,  $n=11$ ).

## 1 Introduction

Non-rigid registration algorithms have recently been used for quantifying change in volume of structures over time, and for quantifying differences between members of a cohort. One approach is to delineate a structure of interest from one image, and use the deformation field calculated by non-rigid registration of that image to a second image to delineate the same structure in the second image [2]. This approach is sometimes called segmentation propagation [3, 4], and is illustrated in Figure 1. Most non-rigid registration algorithms are very sensitive to differences in intensities between images, or to shading artefacts. Non-rigid algorithms that optimise an information theoretic similarity measure such as normalised mutual information are less likely to be sensitive to these effects.

Here we apply the non-rigid registration algorithm devised by Rueckert [5] to study a group of five adult patients being treated with growth hormone replacement therapy, and a group of six volunteers. This group was previously studied using rigid body registration and visual assessment of difference images [6], and that study determined that the greatest change in the patient images was a reduction in the volume of the lateral ventricles. We demonstrate that the non-rigid registration algorithm is able to quantify small changes in volume with

high precision, and also validate the results it produces by comparing them to a visual assessment score previously obtained for the same subjects.

The novelty of this work is the use of segmentation propagation to quantify very small changes in clinical serial MR images, and the comparison of these measurements with results of a blinded visual assessment of difference images for the same subjects. We use a generic atlas and therefore do not require subject-specific segmentation. In related work, the ability of the same algorithm to recover large deformations was validated using a biomechanical model [7].

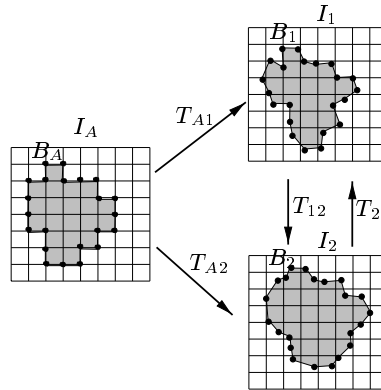


**Fig. 1.** Principle of segmentation propagation.  $I_A$  represents the atlas image with a segmented structure,  $B_A$ , defined by a connected set of boundary points at voxel locations, shown as dots and lines.  $I_1$  and  $I_2$  represent the baseline and repeat images of the patient. Non-rigid registration of  $I_A$  to  $I_1$  and  $I_2$  produces the transformations  $T_{A1}$  and  $T_{A2}$ . Registration of  $I_1$  and  $I_2$  produces the transformations  $T_{12}$  and  $T_{21}$ . Image  $I_A$  is transformed by  $T_{A1}$  and  $T_{A2}$  into the space of  $I_1$  and  $I_2$  which results in propagated structures  $B_1$  and  $B_2$ . Because a transformation results generally in translations of boundary points by a non-integer number of voxels, the transformed set of boundary points does not, in general, coincide with the voxel locations of  $I_1$  and  $I_2$ .

### 1.1 Review of brainweb simulated normal brain image

The brainweb image is available from the McConnell brain imaging centre, Montreal Neurological Institute. It was created by first registering 27 (1mm isotropic voxels)  $T_1$  weighted gradient echo scans of a normal volunteer [1]. These registered images were then corrected for RF inhomogeneity and intensity averaged to produce a high SNR image. This image was then classified into five tissue types: white matter, grey matter, CSF, fat, background; first automatically using a clustering algorithm and then by expert manual editing [1].

## 1.2 Review of Rueckert’s non-rigid registration algorithm

The non-rigid registration algorithm [5] we use here was designed for the registration of dynamic contrast enhanced MR breast images acquired only a few minutes apart. The algorithm uses a free-form deformation (FFD) to model local deformation. The FFD is constructed from a 3D tensor product of B-splines, and deformation is achieved by translating control points while optimising a cost function consisting of two terms: a measure of image similarity (normalised mutual information), and a regularization term (weighted by  $\lambda$ ) that penalises high bending energy deformations. B-splines have compact support so moving one control point only affects the spline coefficients in a local neighbourhood and efficiently models local deformations. The degree of smoothness can be controlled by adjusting the control point spacing. Because B-splines are inherently smooth the deformation energy is typically low, hence, here we ignore the regularization term (i.e.  $\lambda = 0$ ). The algorithm’s optimisation involves translating the control points in steps along the direction of maximum gradient until either the magnitude of the gradient of the cost function is less than or equal to a threshold (Epsilon, set to zero here) or pre-specified number of iterations is exceeded. Then the step size is decreased by a factor of two and the process continues.

## 2 Materials and methods

### Clinical data and atlas

The clinical growth hormone dataset consists of three serial  $T_1$  weighted MR scans of six volunteers and five growth hormone deficient patients with an inter-scan interval of three months. To estimate measurement precision we also acquired three MR scans of another volunteer with the same MR sequence as the patients, but with an inter-scan interval of less than five minutes. Our atlas (registration source image) is based on the brainweb normal brain image without added noise [1] – see review in section 1.1. To reduce image resampling error during affine registration this was interpolated with a Hanning windowed sinc kernel (radius 6 zero crossings) from  $1 \times 1 \times 1$ mm to the same voxel dimension as the clinical data,  $1 \times 1 \times 1.8$ mm. We use the brainweb supplied CSF classification to define the lateral ventricles, as illustrated in Figure 2. To facilitate the measurement of volume (change) this ventricular segmentation was converted to a binary mask image (background voxels = 0, ventricular voxels = 1000).

### Registration and volume measurement strategy

Registration was performed as a two stage process. First global motion and gross differences in head size were compensated for by the affine (12 degrees of freedom) registration algorithm devised by Studholme [8]. Because of large differences in orientation between the atlas image and the subject images, starting estimates within approximately 5mm and 5 degrees were interactively provided prior to affine registration. Secondly, local deformation was calculated using Rueckert’s

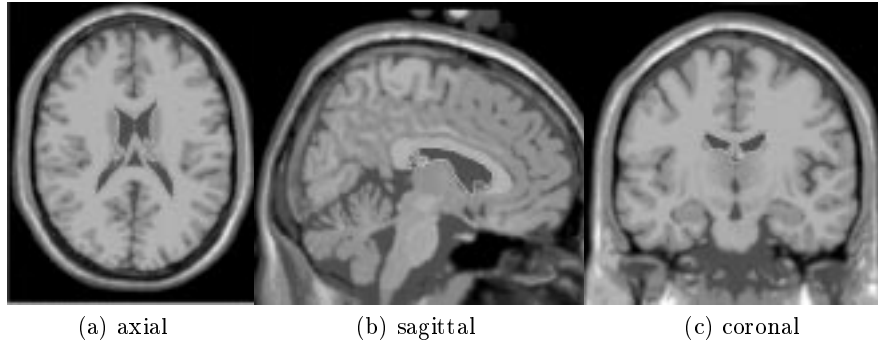


**Fig. 2.** Atlas brain image ( $1 \times 1 \times 1$  mm voxels) with accurate ventricular segmentation – outlined in white. Brainweb images supplied by McGill university, Montreal [1].

algorithm [5] (reviewed in section 1.2), first with a coarse grid (10mm control point spacing) then with a fine grid (5mm control point spacing). The full brain image was used for the coarse grid registration. For the fine grid registration, a region of interest (ROI) was defined surrounding the ventricles using the ventricular outline from the coarse grid registration solution dilated by 7mm to include a boundary layer at least one control point thick around the ROI, see Figure 3(a). Only voxels in this region were used for the fine grid registration, substantially reducing the execution time. For one patient with elongated ventricles, the dilation was increased as shown in Figure 3(b). To reduce the algorithm's

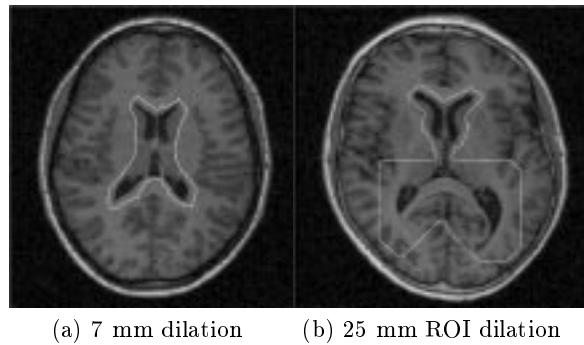


**Fig. 3.** (a) Example of the atlas ventricles dilated by 7 mm and mapped to the space of a patient image. (b) Extra dilation (25 mm) for the patient with elongated ventricles to compensate for the larger deformation.

sensitivity to noise, especially at the fine control point spacing, the images were low-pass filtered with a Gaussian ( $\sigma = 0.5$  voxels).

Ventricular volume (change) was measured by transforming, using linear interpolation, the ventricular binary mask into the space of the subject images using the deformation field calculated by non-rigid registration. Linear interpolation allowed the partial volume of the transformed boundary voxels to be calculated to sub-voxel accuracy, as illustrated in Figure 4. The volume of the mask in the transformed space was calculated by summing the voxel intensities and dividing by 1000 to give an estimate with a rounding error  $\leq 0.05\%$ .



**Fig. 4.** Schematic 1D diagram illustrating volume estimation by linear interpolation of a binary image. Shown in (a) is a voxel of unit intensity with neighbours of zero intensity. Translating one edge by 0.5 voxels increases the volume by 50%, shown as a dark grey region in (b). The neighbouring voxel is interpolated with an intensity of half a unit (c). Hence the measured volume will be 1 voxel in (a) and 1.5 voxels in (c).

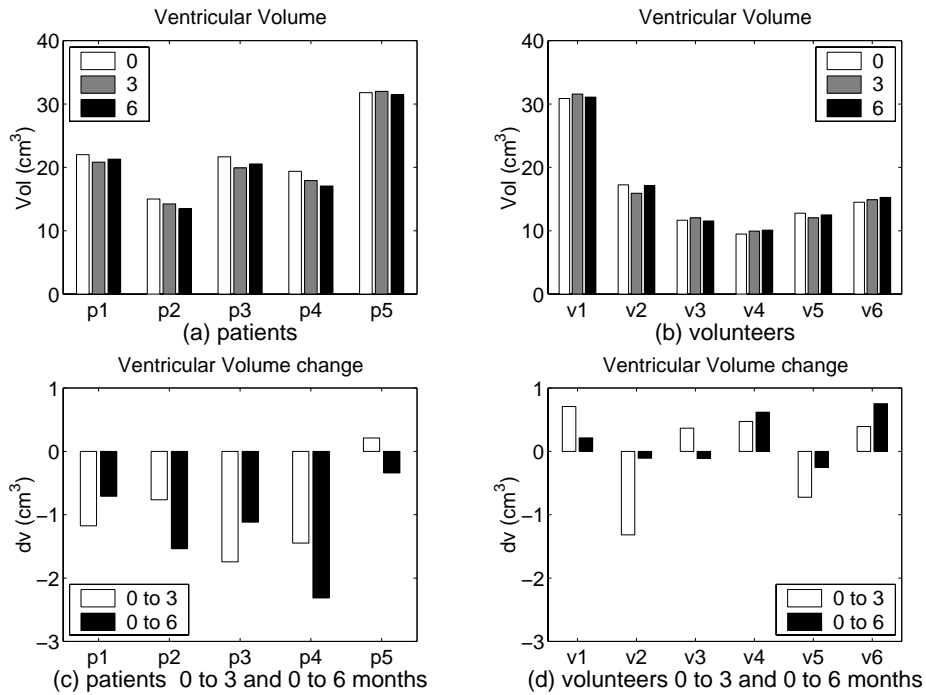
### 3 Results

The measured ventricular volume for the three consecutive volunteer scans was 26.58cc, 26.49cc, 26.50cc which gave a measurement precision of  $\sigma = 0.05\text{cc}$  based on three consecutive scans.

The mean ventricular volume and volume change for the growth hormone study subjects at the 0, 3 and 6 months timepoints is shown in Table 1. Over six months there was a mean 1.2cc (5.5%) decrease in ventricular volume for the patient group compared to a 0.18cc (1.1%) increase for the controls. To test whether the volume change measurements for the two groups differed significantly, the Wilcoxon rank sum test (Matlab, Mathworks Inc, Natick, MA, USA) was used with the null hypothesis that there was no difference between the groups. This gave  $p = 0.013$  (5% significance) for the 0 and 3 month scans and  $p = 0.001$  (1% significance) for the 0 and 6 month scans. The  $p$ -values for both pairs of timepoints was  $p = 0.0016$ , which compares with  $p = 0.0001$  found in our previous study involving qualitative ranking of difference images using a seven point scale [6]. To further compare the volume change measurements with those from the previously published study, we calculated the rank correlation coefficient ( $\rho$ ), this gave  $\rho = 0.76$  for zero to three months,  $\rho = 0.72$  for zero to 6 months, and  $\rho = 0.67$  overall. The  $\rho$  values indicate a significant correlation with the previously published visually assessment results at the 5% level, see [9] for  $n = 11$ . Figure 5 shows graphically the ventricular volume and volume change at the 0, 3 and 6 month timepoints for each of the eleven subjects.

**Table 1.** Mean (std) measured ventricular volume (cc) for patients and volunteers.

Mean (stdev) ventricular volume (cc)			
	timepoint		
group	0 months	3 months	6 months
patients	21.96 (6.16)	20.98 (6.66)	20.76 (6.73)
volunteers	16.08 (7.70)	16.06 (7.90)	16.27 (7.69)
Mean (stdev) of ventricular volume change (cc)			
	timepoints		
group	0 to 3 months	0 to 6 months	overall
patients	-0.98 (0.76)	-1.20 (0.76)	-1.09 (0.73)
volunteers	-0.02 (0.81)	0.18 (0.42)	0.08 (0.62)

**Fig. 5.** Ventricular volume for the 11 subjects in the clinical growth hormone study. (a) and (b) refer to the measured ventricular volume for the 6 volunteers and 5 growth hormone patients at the three timepoints respectively. (c) and (d) refer to the change in ventricular volume from 0 to 3 months and from 0 to 6 months for growth hormone patients and volunteers respectively.

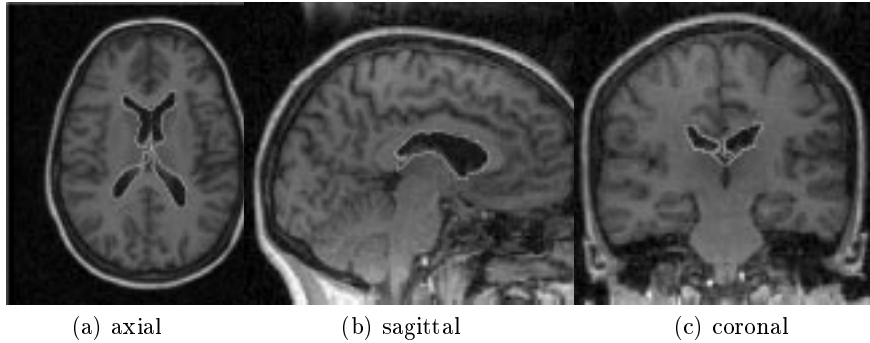


**Fig. 6.** Example of segmentation propagation for patient 1. The boundary of the propagated ventricles is shown outlined in white.

## 4 Discussion and conclusions

A key strength of Rueckert’s non-rigid registration algorithm [5] is that it uses the mutual information (NMI) similarity measure whereas other non-rigid algorithms [10,11] are based on intensity differences. Mutual information has the capability of registering images with non-linearly related voxel intensities. As a result, accurate registration of images that are derived from different scanners and images that are not corrected for intensity inhomogeneity is possible. So a generic brain atlas can be used without needing to acquire and segment extra volunteer images, as was required in previous work (e.g.[3]).

In this paper we have demonstrated that this approach is precise when applied to consecutive scans of a single subject ( $\sigma < 0.05\text{cc}$ ) and that small changes of brain ventricular volume ( $\approx 1\text{cc}$ ) can be quantified by segmentation propagation using the Rueckert non-rigid registration algorithm. This is the first time that a non-rigid registration algorithm based on optimisation of mutual information has been shown to detect volume changes of this magnitude. These measurements are sufficiently accurate to significantly ( $p \approx 0.01$ ) determine ventricular volume change for a group of five growth hormone patients compared to a group of six normal subjects. We have been able to validate the algorithm by demonstrating high correlation ( $\rho \approx 0.7$ ,  $n = 11$ ) between these results and those previously reported from ranking of differences images after rigid registration of the same images [6].

Although our results indicate high precision for one volunteer, and the set of measurements correlate with the previously published ones, the error appears to be larger than this precision value would suggest for individual cases. In particular, the measurements for volunteers v2 and v5, see Figure 5, indicate volume decreases of up to 1cc. Such decreases are inconsistent with the previous published results and implausible biologically and are most likely to be the result of registration error. Further improvements to the registration algorithm would probably reduce these errors.

## Acknowledgements

We are grateful for Philips Medical Systems EasyVision advanced development for funding this work, to Daniel Rueckert for the use of his software, and to our colleagues in the Computational Imaging Science Group, led by Prof. David Hawkes, where the work was carried out. We are also grateful to the McConnell Brain Imaging Centre (BIC) Montreal Neurological Institute for the use of their brainweb simulated MR image.

## References

1. D. L. Collins, A. P. Zijdenbos, V. Kollokian, J. G. Sled, N. J. Kabani, C. J. Holmes, A. C. Evans: Design and construction of a realistic digital brain phantom. *IEEE Trans on Medical Imaging* **17** (1998) 463–468
2. Bajcsy, R., Kovacic, S.: Multiresolution elastic matching. *Computer Vision, Graphics and Image Processing* **46** (1989) 1–21
3. B. M. Dawant, S. L. Hartmann, J. P. Thirion, F. Maes, D. Vandermeulen, P. Demaerel: Automatic 3-D segmentation of internal structures of the head in MR images using a combination of similarity and free-form transformations: Part I, methodology and validation on normal subjects. *IEEE Trans on Medical Imaging* **18** (1999) 909–916
4. G. Calmon, N. Roberts: Automatic measurement of changes in brain volume on consecutive 3D MR images by segmentation propagation. *Magnetic Resonance Imaging* **18** (2000) 439–453
5. D. Rueckert, L. I. Sonoda, C. Hayes, D. L. G. Hill, M. O. Leach, D. J. Hawkes: Non-rigid registration using free-form deformations: Application to breast MR Images. *IEEE Trans on Medical Imaging* **18** (1999) 712–721
6. E. R. E. Denton, M. Holden, E. Christ, J. M. Jarosz, D. Russell-Jones, J. Goodey, T. C. S. Cox, D. L. G. Hill: The identification of cerebral volume changes in treated growth hormone deficient patients using serial 3-D MR image processing. *Journal of Computer Assisted Tomography* **24** (2000) 139–145
7. Schnabel, J.A., Tanner, C., Smith, A.C., Leach, M.O., Hayes, C., Degenhard, A., Hose, R., Hill, D.L.G., Hawkes, D.J.: Validation of non-rigid registration using Finite Element Methods. In: Proc. 17th Int. IPMI 2001 Conf. Vol LNCS 2082, Springer Verlag (2001) 344–357
8. C. Studholme, D. L. G. Hill, D. J. Hawkes: Automated three-dimensional registration of magnetic resonance and positron emission tomography brain images by multiresolution optimization of voxel similarity measures. *Medical Physics* **24** (1997) 25–35
9. M. Bland: An introduction to medical statistics. Oxford Medical Publications (1995) ISBN: 0-19-262428-8.
10. G. E. Christensen, R. D. Rabbitt and M. I. Miller: Deformable templates using large deformation kinematics. *IEEE Trans on Image Processing* **5** (1996) 1435–1447
11. J.-P. Thirion: Image matching as a diffusion process: an analogy with Maxwell's demons. *Medical Image Analysis* **2** (1998) 243–260